

Table of Contents

1. *General*
2. *Synthesis of 5,10-Dioxo-5,10-dihydropyrido[3,4-g]isoquinoline*
3. *Synthesis of N,N'-dimethy-2,6-diaza-9,10-anthraquinonediium bistetrafluoroborate*
4. *General procedure for reduction of N,N'-dimethy-2,6-diaza-9,10-anthraquinonediium bistetrafluoroborate*
5. *X-ray Experimental and Tables for Complex $C_{14}H_{14}N_2O_2^{2+} 2Cl^{-}$*
6. *Electrochemical Procedures*

Experimental Procedures

1. *General*

All chemicals and reagents were purchased from commercial sources and used without further purification. TLC plates and silica gel used for column chromatography (60 Å porosity, 40-63 µm particle size, 0.4 g/mL bulk density, 6.0-8.0 pH range, and <7.0% residual water) were purchased from Sorbtech. The NMR spectra were obtained on 400 MHz and 500 MHz Varian instruments. Hydrogen peroxide test strips (0-100 ppm) were purchased from Indigo Instruments (SKU: 33815-P100; Lot # 160804) and used for all peroxide measurements. The absorbance titrations were performed on a Biotek Cytation 3 Microplate Reader using Costar 96-well plates (#3915).

2. *Synthesis of 5,10-Dioxo-5,10-dihydropyrido[3,4-g]isoquinoline¹*

In an argon-flushed flask 8.5 mL (60.48 mmol) of diisopropylamine were combined with 4.0 mL (21.81 mmol) of hexamethylphosphorus triamide and 70 mL of anhydrous tetrahydrofuran (864 mM in diisopropylamine). The solution was cooled in a dry ice/acetone bath to -78°C and 23 mL of a 2.5 M solution of n-butyllithium in hexanes (57.5 mmol of n-butyllithium) were then added by cannula transfer. This was allowed to stir for 5-10 minutes and then a solution of 3.2 mL (19.03 mmol) of N,N'-diethylnicotinamide in 5 mL of anhydrous tetrahydrofuran (3.806 M in nicotinamide) were added dropwise. The dry ice in the cold bath was replenished and this was allowed to stir overnight, gradually rising to room temperature. After 20 hours the reaction was quenched with 100 mL of water and extracted sequentially with diethyl ether (3x60 mL) and dichloromethane (3x60 mL). The collected dichloromethane extract was dried over sodium sulfate and concentrated under reduced pressure to yield 0.5050 g of crude product. Purification of this by normal-phase silica gel column chromatography (1:1 hexanes/ethyl acetate) gave 0.2495 g of pure DAAD (12%). NOTE: this eluent was not the optimal choice of mobile phase, as the product crashed out on the column. Collected spectra were in agreement with those published in the literature.

3. *Synthesis of N,N'-dimethy-2,6-diaza-9,10-anthraquinonediium bistetrafluoroborate²*

0.2495 g (1.187 mmol) of DAAD were combined with 16.5 mL (71.94 mM in DAAD) of nitromethane in an argon-flushed flask. A solution of 0.8791 g (5.943 mmol) of trimethyloxonium tetrafluoroborate in 8.4 mL (699 mM) of nitromethane was then added dropwise, while stirring vigorously at room temperature. After running the reaction for 30 minutes diethyl ether was added, causing the product to precipitate. This was filtered and dried *in vacuo*, yielding 0.4913 g of analytically pure DAAQ (88%).

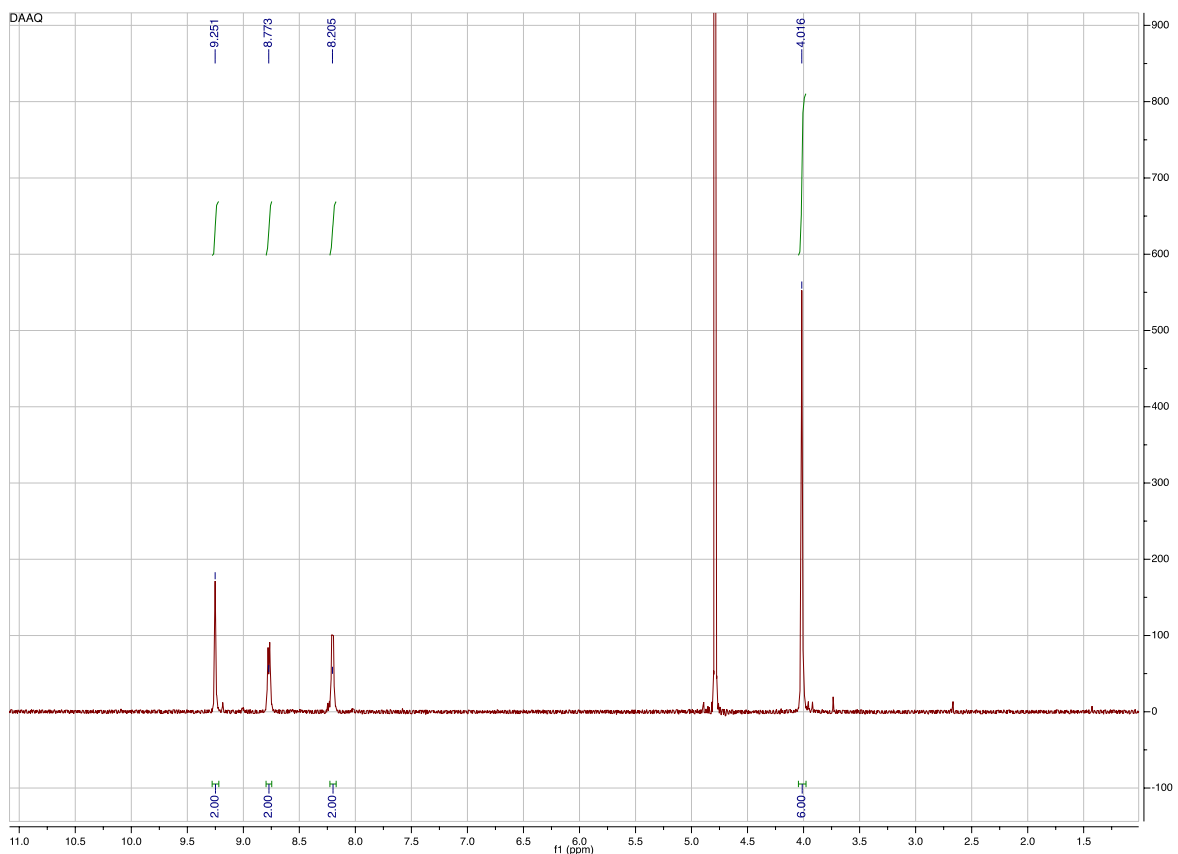


Figure S1. $^1\text{H-NMR}$ of DAAQ in $\text{D}_2\text{O/DCl}$.

4. General procedures for reduction of *N,N'*-dimethy-2,6-diaza-9,10-anthraquinonediium bistetrafluoroborate

For NMR experiments reductions were performed in either pure D_2O or a mixture of D_2O and DCl (deuterated HCl). DAAQ was first dissolved in the deuterated solvent and bisulfite was then added to the solution, reducing the DAAQ. In the lower pH experiments DCl was added in small portions until the NMR showed only the keto-form of DAAQ (as opposed to the gem-diol). After confirming the absence of the gem-diol bisulfite was added, inducing a slow reduction of the quinone. $^1\text{H-NMR}$ s and $^{13}\text{C-NMR}$ s were then acquired of the in situ reduction. For UV/Vis experiments reductions were carried out in pH 4.6 citrate buffered aqueous solutions, to drive the DAAQ equilibrium more towards the keto-form and keep the bisulfite in its mono-anionic state (H_2SO_3 $\text{pK}_{\text{a}1} = 1.857$, $\text{pK}_{\text{a}2} = 7.172$). DAAQ was first dissolved in the previously prepared citrate buffer and bisulfite was then added, causing an immediate reduction. UV/Vis spectra were then acquired of the solutions.

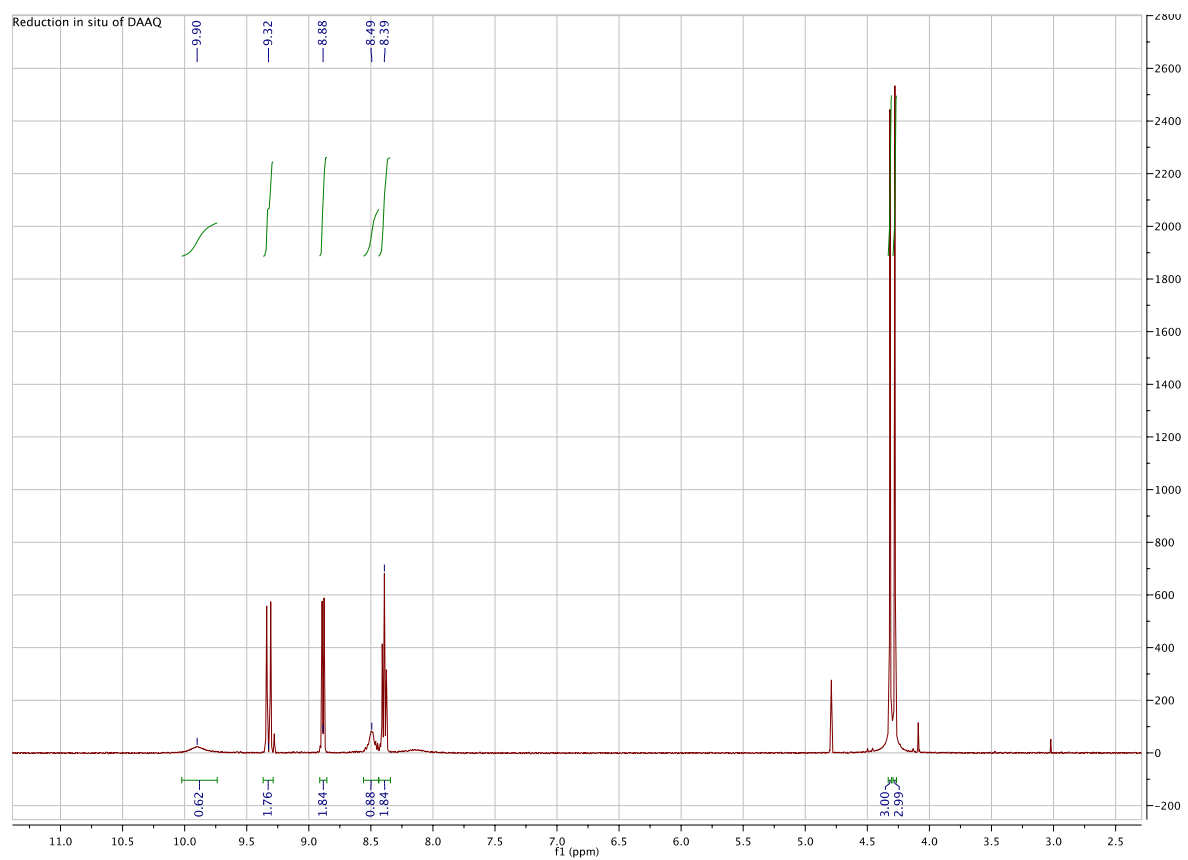


Figure S2. ¹H-NMR of reduction of DAAQ in situ in D₂O/DCI.

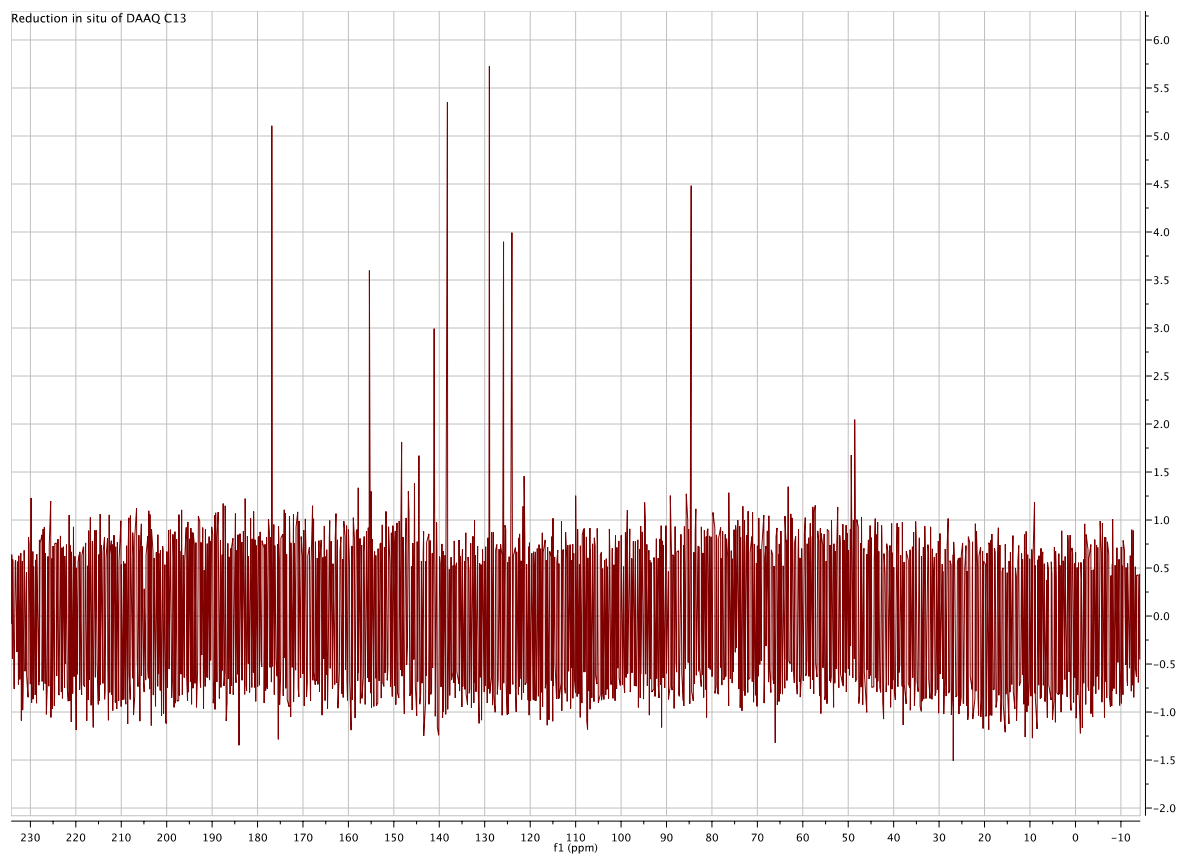


Figure S3. ^{13}C -NMR of reduction of DAAQ in situ in $\text{D}_2\text{O}/\text{DCI}$.



Figure S4. A visual “calibration curve” of known H_2O_2 concentrations. From left to right, a dry (not dipped) test strip, a strip dipped into a 1 ppm H_2O_2 solution, a strip dipped into a 3 ppm H_2O_2 solution, a strip dipped into a 10 ppm H_2O_2 solution, a strip dipped into a 50 ppm H_2O_2 solution that was passed through a silica plug in a pasteur pipette, a strip dipped into a 50 ppm H_2O_2 solution, and a strip dipped into a 100 ppm H_2O_2 solution,

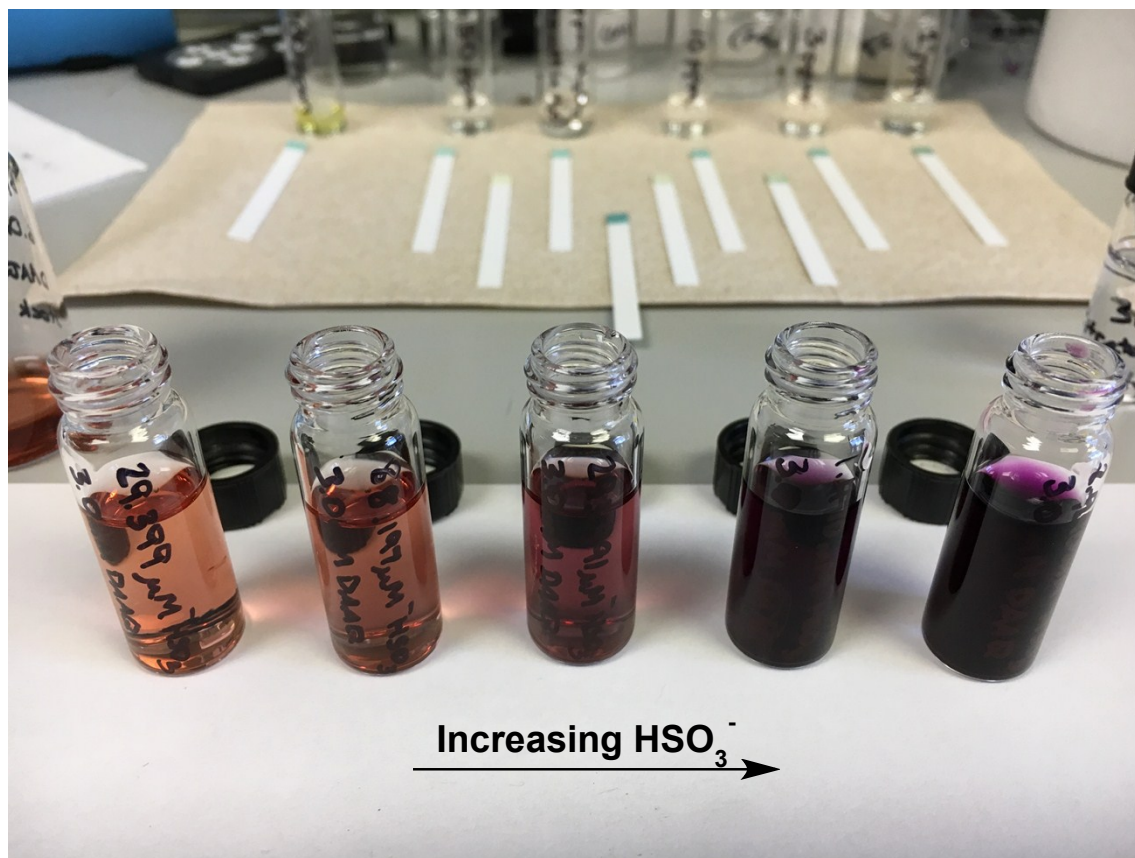


Figure S5. Example of a UV/Vis titration of DAAQ with bisulfite. From left to right, the vials initially contained 0.01, 0.03, 0.1, 0.5, and 1.0 equivalents of bisulfite in pH 4.6 citrate buffer. A solution of DAAQ was added simultaneously to all of the vials (to a final concentration of 3.0 mM DAAQ), the vials were capped and shaken for a few seconds, and the photo was immediately taken.

5. X-ray Experimental and Tables for Complex $C_{14}H_{14}N_2O_2^{2+} 2Cl^{-}$

Crystals grew as red laths by precipitation from D_2O during a NMR experiment. 30.39 mg (73.43 μmol) of DAAQ were combined with 7.71 mg (74.09 μmol) of sodium bisulfite in a mixture of 900 μL of D_2O and 350 μL of 20 wt. % DCl (deuterated HCl) in D_2O , sonicated to allow everything to dissolve, and the 58.74 mM solution was run over the weekend in a 500 MHz Varian NMR spectrometer. When the NMR tube was retrieved from the NMR facility it contained crystals of $DAAQH_2$. The data crystal was cut from a larger crystal and had approximate dimensions; 0.24 x 0.13 x 0.032 mm. The data were collected on an Agilent Technologies SuperNova Dual Source diffractometer using a μ -focus $\text{Cu K}\alpha$ radiation source ($\lambda = 1.5418 \text{ \AA}$) with collimating mirror monochromators. A total of 1143 frames of data were collected using ω -scans with a scan range of 1° and a counting time of 3 seconds per frame with a detector offset of $\pm 40.8^\circ$ and 10 seconds per frame with a detector offset of $\pm 108.3^\circ$. The data were collected at 100 K using an Oxford Cryostream low temperature device. Details of crystal data, data collection and structure refinement are listed in **Table S1**. Data collection, unit cell refinement and data reduction were performed using Agilent Technologies CrysAlisPro V 1.171.37.31.³ The structure was solved by direct methods using SuperFlip⁴ and refined by full-matrix least-squares on F2 with anisotropic displacement parameters for the non-H atoms using SHELXL-2013.⁵ Structure analysis was aided by use of the programs PLATON98⁶ and WinGX.⁷ The hydrogen atoms were calculated in ideal positions with isotropic displacement parameters set to 1.2xUeq of the attached atom (1.5xUeq for methyl hydrogen atoms). The complex sits around a crystallographic inversion center at $\frac{1}{2}, \frac{1}{2}, \frac{1}{2}$.

The function, $\sum w(|F_o|^2 - |F_c|^2)^2$, was minimized, where $w = 1/[(\sigma(F_o))^2 + (0.0987*P)^2 + (0.0596*P)]$ and $P = (|F_o|^2 + 2|F_c|^2)/3$. $R_w(F^2)$ refined to 0.127, with $R(F)$ equal to 0.0429 and a goodness of fit, S , = 1.13. Definitions used for calculating $R(F)$, $R_w(F^2)$ and the goodness of fit, S , are given below.⁸ The data were checked for secondary extinction effects but no correction was necessary. Neutral atom scattering factors and values used to calculate the linear absorption coefficient are from the International Tables for X-ray Crystallography (1992).⁹ All

figures were generated using SHELXTL/PC.¹⁰ Tables of positional and thermal parameters, bond lengths and angles, torsion angles and figures are found elsewhere.

Table S1. Crystal data and structure refinement for DAAQH₂.

Empirical formula	C14 H14 Cl2 N2 O2	
Formula weight	313.17	
Temperature	100(2) K	
Wavelength	1.54184 Å	
Crystal system	triclinic	
Space group	P -1	
Unit cell dimensions	a = 4.4516(10) Å	α = 86.957(9)°.
	b = 6.7274(16) Å	β = 83.772(8)°.
	c = 11.4945(18) Å	γ = 77.680(11)°.
Volume	334.16(12) Å ³	
Z	1	
Density (calculated)	1.556 Mg/m ³	
Absorption coefficient	4.400 mm ⁻¹	
F(000)	162	
Crystal size	0.240 x 0.130 x 0.032 mm ³	
Theta range for data collection	3.870 to 74.173°.	
Index ranges	-? ≤ h ≤ ?, -? ≤ k ≤ ?, -? ≤ l ≤ ?	
Reflections collected	1304	
Independent reflections	1304 [R(int) = ?]	
Completeness to theta = 67.684°	99.4 %	
Absorption correction	Semi-empirical from equivalents	
Max. and min. transmission	1.00 and 0.544	

Refinement method	Full-matrix least-squares on F^2
Data / restraints / parameters	1304 / 0 / 92
Goodness-of-fit on F^2	1.126
Final R indices [$I > 2\sigma(I)$]	R1 = 0.0429, wR2 = 0.1270
R indices (all data)	R1 = 0.0431, wR2 = 0.1273
Extinction coefficient	n/a
Largest diff. peak and hole	0.459 and -0.573 e.Å ⁻³

Table S2. Atomic coordinates ($\times 10^4$) and equivalent isotropic displacement parameters ($\text{\AA}^2 \times 10^3$) for DAAQH₂. $U(\text{eq})$ is defined as one third of the trace of the orthogonalized U^{ij} tensor.

	x	y	z	U(eq)
O1	8245(3)	7588(2)	5889(1)	16(1)
N1	5424(3)	2779(2)	7970(1)	13(1)
C1	6655(4)	6311(3)	5503(2)	13(1)
C2	5678(4)	4686(3)	6162(2)	13(1)
C3	6259(4)	4314(3)	7352(2)	14(1)
C4	3896(4)	1469(3)	7506(2)	16(1)
C5	3186(4)	1750(3)	6383(2)	14(1)
C6	4058(4)	3376(3)	5660(2)	13(1)
C13	6083(5)	2451(3)	9212(2)	19(1)
Cl1	10291(1)	7462(1)	8315(1)	16(1)

Table S3. Bond lengths [Å] and angles [°] for DAAQH₂.

O1-C1	1.343(2)	C3-H3	0.95
O1-H1O	0.91	C4-C5	1.356(3)
N1-C3	1.319(2)	C4-H4	0.95
N1-C4	1.382(2)	C5-C6	1.433(3)
N1-C13	1.483(2)	C5-H5	0.95
C1-C6#1	1.402(3)	C6-C1#1	1.402(3)
C1-C2	1.415(3)	C13-H13A	0.98
C2-C3	1.419(2)	C13-H13B	0.98
C2-C6	1.430(3)	C13-H13C	0.98
C1-O1-H1O	118.8	C5-C4-H4	120.0
C3-N1-C4	122.14(16)	N1-C4-H4	120.0
C3-N1-C13	119.52(15)	C4-C5-C6	120.63(17)
C4-N1-C13	118.32(16)	C4-C5-H5	119.7
O1-C1-C6#1	116.40(16)	C6-C5-H5	119.7
O1-C1-C2	125.75(16)	C1#1-C6-C2	120.66(17)
C6#1-C1-C2	117.84(17)	C1#1-C6-C5	121.38(17)
C1-C2-C3	120.77(17)	C2-C6-C5	117.96(17)
C1-C2-C6	121.49(17)	N1-C13-H13A	109.5
C3-C2-C6	117.73(16)	N1-C13-H13B	109.5
N1-C3-C2	121.50(16)	H13A-C13-H13B	109.5
N1-C3-H3	119.2	N1-C13-H13C	109.5

C2-C3-H3	119.2	H13A-C13-H13C	109.5
C5-C4-N1	120.01(16)	H13B-C13-H13C	109.5

Symmetry transformations used to generate equivalent atoms:

#1 -x+1,-y+1,-z+1

Table S4. Anisotropic displacement parameters ($\text{\AA}^2 \times 10^3$) for DAAQH₂. The anisotropic displacement factor exponent takes the form: $-2\pi^2 [h^2 a^{*2} U^{11} + \dots + 2 h k a^* b^* U^{12}]$

	U ¹¹	U ²²	U ³³	U ²³	U ¹³	U ¹²
O1	17(1)	14(1)	20(1)	-1(1)	-5(1)	-8(1)
N1	10(1)	12(1)	18(1)	-2(1)	-1(1)	-2(1)
C1	7(1)	11(1)	21(1)	-4(1)	-2(1)	-1(1)
C2	8(1)	10(1)	20(1)	-3(1)	0(1)	0(1)
C3	9(1)	12(1)	20(1)	-5(1)	-1(1)	-1(1)
C4	11(1)	13(1)	23(1)	-1(1)	-1(1)	-3(1)
C5	9(1)	11(1)	24(1)	-2(1)	-1(1)	-3(1)
C6	8(1)	11(1)	21(1)	-3(1)	1(1)	0(1)
C13	21(1)	17(1)	18(1)	-2(1)	-3(1)	-3(1)
Cl1	15(1)	14(1)	21(1)	-4(1)	-3(1)	-6(1)

Table S5. Hydrogen coordinates ($\times 10^4$) and isotropic displacement parameters ($\text{\AA}^2 \times 10^{-3}$) for DAAQH₂.

	x	y	z	U(eq)
H1O	8863	7376	6622	24
H3	7272	5191	7711	16
H4	3342	370	7974	19
H5	2099	861	6073	17
H13A	7242	3450	9412	28
H13B	7310	1074	9326	28
H13C	4133	2613	9718	28

Table S6. Torsion angles [$^\circ$] for DAAQH₂.

O1-C1-C2-C3	2.2(3)
C6#1-C1-C2-C3	-178.51(14)
O1-C1-C2-C6	-178.36(16)
C6#1-C1-C2-C6	1.0(3)
C4-N1-C3-C2	-1.1(3)
C13-N1-C3-C2	179.97(15)
C1-C2-C3-N1	-178.49(15)
C6-C2-C3-N1	2.0(2)

C3-N1-C4-C5	-0.5(3)
C13-N1-C4-C5	178.37(16)
N1-C4-C5-C6	1.2(3)
C1-C2-C6-C1#1	-1.0(3)
C3-C2-C6-C1#1	178.50(14)
C1-C2-C6-C5	179.23(15)
C3-C2-C6-C5	-1.3(2)
C4-C5-C6-C1#1	179.94(16)
C4-C5-C6-C2	-0.3(3)

Symmetry transformations used to generate equivalent atoms:

#1 -x+1,-y+1,-z+1

Table S7. Hydrogen bonds for DAAQH₂ [Å and °].

D-H...A	d(D-H)	d(H...A)	d(D...A)	<(DHA)
O1-H1O...Cl1	0.91	2.12	3.0185(14)	169.5
C3-H3...Cl1	0.95	2.41	3.3519(18)	170.7
C4-H4...Cl1#2	0.95	2.60	3.4586(19)	150.4
C13-H13A...Cl1#3	0.98	2.93	3.427(2)	112.6
C13-H13B...Cl1#4	0.98	2.76	3.620(2)	147.1
C13-H13C...Cl1#5	0.98	2.84	3.786(2)	162.8

Symmetry transformations used to generate equivalent atoms:

#1 -x+1,-y+1,-z+1 #2 x-1,y-1,z #3 -x+2,-y+1,-z+2

#4 x,y-1,z #5 -x+1,-y+1,-z+2

6. Electrochemical Procedures

Electrochemical experiments were carried out in a nitrogen atmosphere glovebox using 0.1 M N-tetrabutylammonium hexafluorophosphate (TBAPF₆) as supporting electrolyte dissolved in anhydrous acetonitrile (MeCN) stored over molecular sieves. TBAPF₆ was recrystallized three times from hot ethanol before drying for 72 hours under active vacuum. A conventional three-electrode cell composed of a Pt button working electrode (2mm diameter), a Ag/Ag⁺ (0.01 M AgNO₃ in 0.1 M TBAPF₆/MeCN) non-aqueous reference electrode, and a Pt wire counter electrode was used for all electrochemical experiments. Cyclic voltammograms were recorded using GPES software with an Autolab PGSTAT30 Potentiostat. All potentials were reported versus the Ferrocene/Ferrocenium (Fc/Fc⁺) redox couple. Ferrocene was sublimated at 95°C prior to use. Anthraquinone (AQ) was used as received from Aldrich.

Electrochemical cells were assembled by adding AQ or N,N'-dimethyl-2,6-diaza-9,10-anthraquinonediium (DAAQ) tetrafluoroborate powder to a solution of freshly prepared 0.1 M TBAPF₆ in MeCN. AQ was cycled from 0 to -2.4 V vs Ag/Ag⁺ at 50 mV/s. DAAQ was cycled from 0.25 to -0.43 V vs Ag/Ag⁺ at 5 mV/s. These potential windows were chosen to highlight the redox activity of AQ and DAAQ respectively. The scan rate for DAAQ was reduced to capture the oxidation peaks separately. Due to the ease of oxidation and small energetic difference, the oxidation peaks do not resolve from one another at faster scan rates.

References

- 1 V. Bolitt, C. Mioskowski, S. P. Reddy and J. R. Falck, *Synthesis*, **1988**, 5, 388-389.
- 2 A. Thangavel, I. A. Elder, C. Sotiriou-Leventis, R. Dawes and N. Leventis, *J. Org. Chem.*, **2013**, 78, 8297-8304.
- 3 CrysAlisPro. Agilent Technologies (2013). Agilent Technologies UK Ltd., Oxford, UK, SuperNova CCD System, CrysAlicPro Software System, 1.171.37.31.
- 4 SuperFlip. Palatinus, L. Chapuis, G. (2007). *J. Appl. Cryst.* 40, 786-790.
- 5 Sheldrick, G. M. (2008). SHELXL-2013. Program for the Refinement of Crystal Structures. *Acta Cryst.*, A64, 112-122.
- 6 Spek, A. L. (1998). PLATON, A Multipurpose Crystallographic Tool. Utrecht University, The Netherlands.
- 7 WinGX 1.64. (1999). An Integrated System of Windows Programs for the Solution, Refinement and Analysis of Single Crystal X-ray Diffraction Data. Farrugia, L. J. *J. Appl. Cryst.* 32, 837-838.
- 8 $R_w(F^2) = \{\sum w(|F_o|^2 - |F_c|^2)^2 / \sum w(|F_o|^4)\}^{1/2}$ where w is the weight given each reflection.
 $R(F) = \sum (|F_o| - |F_c|) / \sum |F_o|$ for reflections with $F_o > 4(\sigma(F_o))$.
 $S = [\sum w(|F_o|^2 - |F_c|^2)^2 / (n - p)]^{1/2}$, where n is the number of reflections and p is the number of refined parameters.
- 9 International Tables for X-ray Crystallography (1992). Vol. C, Tables 4.2.6.8 and 6.1.1.4, A. J. C. Wilson, editor, Boston: Kluwer Academic Press.
- 10 Sheldrick, G. M. (1994). SHELXTL/PC (Version 5.03). Siemens Analytical X-ray Instruments, Inc., Madison, Wisconsin, USA.